LBNL-41298

ERNEST ORLANDO LAWRENCE
BERKELEY NATIONAL LABORATORY

Departure from the Hadronic Scenario at CERN SPS

Grażyna Odyniec

Nuclear Science Division

January 1998

Invited paper
presented at the
Fifth Rio de Janeiro
International Workshop
on Relativistic Aspects of
Nuclear Physics,
Rio de Janeiro, Brazil,
August 27–29, 1997
and to be published in
the Proceedings

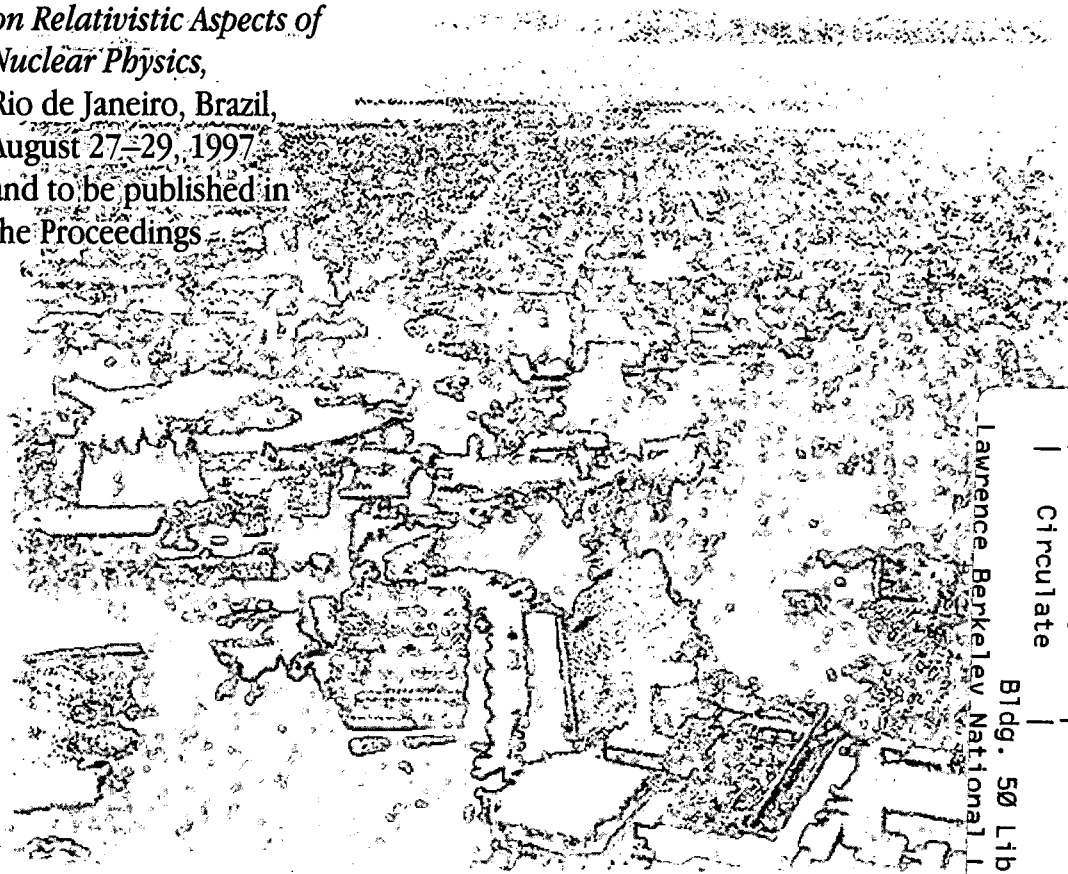

DISCLAIMER

LBNL-41298

Departure from the Hadronic Scenario at CERN SPS

Grażyna Odyniec

Nuclear Science Division
Ernest Orlando Lawrence Berkeley National Laboratory
University of California
Berkeley, California 94720

January 1998

This work was supported by the Director, Office of Energy Research, Office of Basic Energy Sciences, Nuclear Sciences Division, of the U.S. Department of Energy under Contract No. DE-AC03-76SF00098.

Departure from the Hadronic Scenario at CERN SPS

Grażyna Odyniec
Nuclear Science Division
Ernest Orlando Lawrence Berkeley National Laboratory
University of California
Berkeley, California 94720

Abstract:

A review of results from heavy ion experiments at CERN SPS is presented, with an emphasis on the data from Pb induced interactions. Special focus is put on the most significant surprises: anomalous J/Ψ suppression, change in the spectral shapes of e^+e^- mass distributions in the vector meson domain, and enhanced strange hadron production. Implications of these findings for understanding collision dynamics and, in particular, their role in the search for the new phase of matter, are discussed.

1. Introduction

Recent results from Pb on Pb collisions at CERN SPS have confirmed [1], beyond any doubt, previous "hints" of new physics emerging from the analysis of S+S interactions at 200 GeV/c.

The state of the art model of strong interacting matter, lattice QCD, predicts the phase transition to quark-gluon plasma phase at a critical temperature of 150-160 MeV where the energy density $\varepsilon_C \sim 1$ GeV/fm^3 [2]. Such a transition would result in a "critical" jump occurring in bulk matter concerning the energy density, specific heat, magnitude of the quark mass scale (quark condensates), etc. In the first approximation very similar conditions were present at the beginning of the Universe, towards the end of the nanosecond era.

In the experimental study of quark gluon plasma properties high energy nuclear collisions play a unique role. They allow the creation of a "macroscopic" (in comparison to the characteristic scale of strong interaction ~1fm) space-time region with high energy density in the laboratory. The volume and energy density are controlled by the sizes of the colliding nuclei and their collision energy. Recent data on central Pb+Pb

collisions at the highest energy available in the laboratory (CERN SPS: $\sqrt{s} \cong 20$ GeV) indicate that matter with an energy density of several GeV/fm^3 is created at the early stage of the collision [3], which appears to far exceed the critical energy density ε_c. The transient existence of a quark-gluon plasma in the collision is expected to modify the evolution of the system compared to a scenario of confined hadronic matter. Some new results from analysis of Pb+Pb interactions fall into a common pattern that could not be explained within a hadronic scenario, but may very well signal the features of a QCD phase transition.

In the first part of this overview, we shall briefly outline the complexity of the analysis and experimental techniques. Secondly, we will describe global features of central Pb+Pb collisions. The main body of this paper will focus on the anomalous J/Ψ suppression, change in the spectral shapes of e^+e^- mass distributions in the vector meson domain and on the enhancement of strange particle production. Lastly, we will present one of the possible non-conventional interpretations of the discussed results.

2. Experimental Techniques and Analysis

All seven major fixed-target heavy ion experiments at the SPS address different physics observables, and therefore use quite different experimental techniques. NA45 and NA38/50 focus on lepton pairs: e^+e^- (NA45) [4] and $\mu^+\mu^-$ (NA38/50) [5]. WA85/94/97 [6] investigates multistrange hyperon production. NA52 concentrates on a strangelets search [7]. WA98 studies direct photon signals [8], and NA44 examines hadronic correlations [46]. NA35/49 [9] has a particularly large p_t - y coverage and, therefore, has the ability to determine many global observables. All these experiments deal very well with the enormously high multiplicity of events (in Pb+Pb collisions - up to few thousand particles in the final state) either by extremely high space point resolution over a large volume of the detector (e.g. TPC's in NA49) or by extreme selectivity of the studied signal (e.g. muon pairs in NA38/50, or restricted to exotic values of the charge-to-mass ratio in the strangelet study of NA52).
Figure 2 illustrates the complexity of a typical Pb+Pb raw event recorded in the NA49 Time Projection Chamber (TPC). The upper part of the Fig.1 visualizes a large TPC subvolume (~ 30 cm depth), whereas the lower part much smaller subvolume (of ~ 5 cm of depth) extracted offline from the full event (upper part of the picture). The ability to divide an entire three-dimentional picture of the collision, stored in the computer memory (full depth of the detector), into smaller slices with the complexity appropriate for the applied pattern recognition algorithm and tracking software (dictated mainly by the track density), allowed highly efficient analysis of these events. It has been demonstrated that the space point resolution in the detector is adequate and that the track recorded density is clearly manageable by the software (see Fig.1 and [9]). As an example of a high quality analysis performed on that data, we present in Fig.2 the invariant-mass distributions of neutral strange particles Λ, $\overline{\Lambda}$ and K^0 analyzed by pattern recognition of their secondary decay vertices.

3. Global Features of Pb on Pb Collisions.

From early results of CERN experiments with S beams, we learned that a significant fraction of the individual longitudinal energy becomes degraded during the interaction (due to elastic and inelastic collisions at the microscopic level) and deposited into the reaction volume. This became even more apparent with the heavier beams. Fig.3 shows the net baryon distribution measured by the NA49 for central Pb+Pb collisions as a function of rapidity, together with the net baryon distribution for central S+S collisions measured by the NA35 experiment [9,10]. The Pb+Pb system exhibits considerably greater stopping than S+S, indicated by the much larger fraction of baryons at mid-rapidity. In fact, for Pb+Pb the rapidity distribution is approximately flat over two units around mid-rapidity and is somewhat narrower than the net baryon yield in S+S collisions, scaled for comparison by the ratio of participant nucleons in both systems. Increased available energy is not used for the production of negatively charged hadrons (90% of which are π^-). Fig.4 shows that rapidity distribution of negative hadrons measured for central Pb+Pb collisions by NA49 and for S+S (scaled) by NA35 resemble each other very closely over the entire range of rapidity. The peak at mid-rapidity is broader than would result from an isotropic "fireball" at T=160MeV, reflecting an elongation of the source along the beam direction.

Naturally, the energy deposited into the interaction volume (mid-rapidity in Fig.3 and 4) increases the energy density there. An observed plateau at $2<y<4$ suggests that the boost-invariant dynamics of the Bjorken picture [11], for a quantitative estimate of the spatial energy density in the primordial interaction volume, may be justified here. This estimate, based on the measured energy density in rapidity space, $dE/d\eta$, [12] and on space-time geometry, results in $\varepsilon \sim 2.8$ GeV/fm^3 for Pb+Pb. This should be sufficient to match (and exceed) the value set by lattice QCD results for the phase transition, even allowing for the uncertainty related to the τ_0 parameter of the Bjorken formula (at present, τ_0=1 fm/c is used rather arbitrarily for the formation time). Interestingly, applying the same procedure to a much lighter system, S+Au, led to the surprisingly close result of ε=2.5 GeV/fm^3. However , one should not forget that the Bjorken estimate represents an average over the total source volume. More detailed calculations [13,14] show that two systems have very different radial density profiles, being rather flat in case of S+Au, where the value of the peak is quite close to the average, and distinctly peaked for Pb+Pb collisions (at its maximum, the energy density distribution for Pb+Pb reaches 3.5 GeV/fm^3). This tentative argument is used sometimes to explain why the anomalous J/Ψ suppression reported by the NA38/50 experiment might be related to a partonic scenario.

4. J/Ψ and Ψ' Production

The idea that charmonium production may be a suitable probe for the plasma phase or deconfinement is already more than 10 years old [15]. At the early stage of the collision, suppression of the J/Ψ and Ψ' resonances is expected from a QCD

mechanism, analogous to Debeye screening in a QED plasma, or from interaction of the charmonia state with the hard gluons present in deconfined matter. Moreover, it has been demonstrated [16] that neither J/Ψ nor Ψ' could be broken up by a hadronic co-moving environment, because hard processes should in general suffer no effect by the later stage of the heavy ion collision. Therefore, J/Ψ and Ψ' suppression, if observed, would provide a relatively "clean" signature (in terms of the interpretation) of a QCD phase transition.

A special experiment was designed to search for experimental evidence of J/Ψ and Ψ' suppression, and indeed, early results from the NA38 reported ~50% suppression of J/Ψ in central S+U collisions, compared to scaling from elementary pp and pA data at the same energy[17].

However, further developments seriously modified the above mentioned arguments. Critical information came from the analysis of pA data. Figure 5 shows a compilation of J/Ψ, Ψ' and χ yields from the E772 [18] and NA38 [5,17] experiments plotted vs an average path length L_A, traversed by a $c\bar{c}$ pair produced in nuclear targets on their way out into free space (L_A=Glauber path length) [19]. Serious attenuation of the yields (Fig.5) is well described by the absorption law (straight line): $S_0=\exp(-n_0\sigma L_A)$ where $n_0= 0.15/fm^3$ is the ground state baryon density and σ = 6.2 mb is the absorption cross section. It is obvious that the same cross section can not describe absorption of J/Ψ and Ψ', since Ψ' is much more weakly bound than J/Ψ, and its radius is about two times larger than that of J/Ψ; therefore, it should break up much more easily, resulting in much stronger attenuation.

There is no clear mechanism explaining this observation; however, tentatively, it was associated with the initial prehadronic $c\bar{c}$ state reacting with cold target matter, before the $c\bar{c}$ pair "dresses up" to J/Ψ or Ψ'. In this picture, what was observed (Fig.5) was interpreted, not as J/Ψ and Ψ' break-up, but rather as break up of their prehadronic, common progenitor. Further explanation followed from a thorough revision of the entire $c\bar{c}$ hadronization mechanism [20], where it was calculated that the cross section of the J/Ψ, Ψ' progenitor state indeed amounts to the same value of ~6 mb [21].

Production of J/Ψ in A+A collisions, studied by the NA38 (S+U) and NA50 (Pb+Pb) experiments, is summarized in Fig.6. The yields are normalized to the underlying Drell-Yan production cross section of $\mu+\mu-$ pairs, which is shown to be completely independent of the colliding system. The relative yields of J/Ψ in p+ (p, d, W, U) and S+U and Pb+Pb are plotted vs average length L_A (as on Fig.5). The data samples for S+U are divided into five centrality intervals using neutral transverse energy measurements. Within the framework of the absorption model, the cross section for dissociation of the $c\bar{c}$ pair by a nucleon is σ_{abs} = (6.2+/-0.7)mb (fit to the NA38 data, shown by a full line on Fig.6). In contrast to the NA38 data, the suppression of J/Ψ in Pb+Pb collisions can not be explained by nuclear absorption alone. When plotted versus L_A, the anomalous suppression appears as a sharp discontinuity from the nuclear absorption mechanism in Pb+Pb collisions. For the lower Pb+Pb centrality bin, corresponding to a moderately large impact parameter, the data point is fully

compatible with the one obtained in S+U central collisions. This implies that no anomalous J/Ψ suppression is observed in peripheral (b>8 fm) Pb+Pb collisions, whereas, in the case of more central Pb+Pb collisions, anomalous suppression keeps increasing with centrality. An additional break-up mechanism thus appears to be present in central Pb+Pb collisions.

It has been calculated [14] that the J/Ψ yield in the most central bins of the NA50 Pb+Pb data is consistent with a completely black, absorptive core volume, of energy density exceeding 3 GeV/fm^3. The remaining J/Ψ yields (less central bins) correspond to the unavoidable surface regions of an equal mass collision (corona effect), where it occurs essentially as in free p+p collisions. The observed anomalous degree of suppression, far beyond the ~6 mb of prehadronization break-up, was tentatively interpreted as a result of creation of the energy density in the core of the Pb+Pb interaction volume, comfortably sufficient for creation of partonic, rather than a hadronic, state.

5. Low-mass Electron Pair Production

Leptons are produced during the entire evolution of the reaction, from the very hot early stage of the collision to the very last moment when freeze-out takes over and hadrons stop interacting. Since they do not re-interact - their mean free path (electromagnetic interactions) is much larger than the size of the interaction volume - leptons are assumed to be reliable messengers of all subsequent stages of the system evolution. Therefore, a careful analysis might be able to unfold the entire space-time history of the collision and, perhaps, even to separate the contributions from the partonic and hadronic stages of the collision.

Figure 7 shows the mass spectra of inclusive e^+e^- pairs in p+Be at 450 GeV/c (left panel) and S+Au at 200 GeV/c (right panel) collisions, measured by the NA45/CERES experiment [22]. A significant excess, about a factor of 5, of low-mass electron pairs is seen in S+Au collisions over the, so called, "cocktail" of known hadronic sources (Dalitz decays of the π^0, η, η', ω and decays of the ρ, ω, and Φ resonances) estimated by scaling from pp collisions [23, 24]. In the case of the proton-induced interactions, the low mass spectra are, within errors, satisfactorily explained by the electron pairs from hadronic decays. The enhancement in Pb+Pb collisions (Fig.8) is very similar in shape to the one observed in S+Au collisions (Fig.7), but its magnitude is about two times smaller, with large statistical and systematic errors, than in the S+Au system. For clarification: the enhancement factor is defined as the ratio of the integral of the data over the integral of the predicted hadronic sources.

The excess in S+Au collisions as confirmed by Pb+Pb data, and a corresponding one observed in the low-mass dimuon spectrum reported by the HELIOS/3 experiment, have triggered intense theoretical activities with the most urgent question being: are we seeing the first indication of the thermal radiation emitted from the dense hadronic matter formed in relativistic ion collisions ? This is not answered yet. Most of the theoretical effort has focused on including in the model calculations some of the mechanisms not present in pp and pA collisions, and, therefore, are not accounted for in

the hadronic "cocktail" approach - but are expected to play a significant role in AA collisions. The collision dynamics have been treated in a variety of ways, including transport models with explicit propagation of baryons and mesons, with the assumption of the thermal equilibrium present [25] and without thermal equilibrium [26,27], standard hydrodynamical models with the formation of thermalized QGP [28,29], models based on a thermalized hadronic gas [29,30], etc.

All calculations led to the same results; they were able to satisfactorily describe the dilepton excess near the ρ/ω mass (a direct consequence of including the pion annihilation channel in the calculations), but they underestimated the NA45 data in the mass region of $0.2 < m_{ee} < 0.5$ GeV/c^2. At the present stage of development, the data in this mass region can be satisfactory described only by introducing a decrease of the meson masses in the high density phase after hadronization (solid line in Fig.9). For the details, see reference 31. The same calculations also well reproduce the low-mass enhancement found in the HELIOS/3 dimiuon data (Fig.9b).

To summarize, the satisfactory description of the low mass dilepton enhancement observed by the NA45 and HELIOS/3 experiments requires an in-medium meson mass treatment that might be interpreted as a signal of the onset of hadronic chiral restoration mass loss in a high density hadronic medium. On the other hand, one is tempted to speculate that it also might be a further direct signal from the partonic phase of the collision, where dilepton enhancement in the lower mass region may result from processes like quark-quark annihilation or quark-gluon Compton scattering, etc.

The present uncertainties in the data, however, are still too large to convincingly rule out, other more conventional, explanations. So, continuation of this analysis, with particular emphasis on reducing systematic errors and providing information on the dependencies of e^+e^- yields on the other variables characterizing system, is very important, as is theoretical work related to the final interpretation of these extremely intriguing results.

6. Strangeness Production

Strangeness production in heavy ion collisions has long been regarded as a sensitive probe of the proximity to chemical equilibrium [32] than the system may achieve. When analyzing particle ratios and yields, one has to concentrate on measurements in full phase space; otherwise, the results are strongly dependent on kinematical regions of the phase space, and the conclusions are not very reliable.

So far, only pion and kaon multiplicities (in 4π) are available for Pb+Pb collisions [33]. The ratio $<\pi>$ per participant is about the same in S+S and Pb+Pb collisions (as discussed in section 3), being larger than the corresponding ratio in nucleon-nucleon interactions. Figure 10 shows the $<K+K>/<\pi>$ ratio for various systems. $<\pi> = 3^* <h^->$ denotes the multiplicity of pions of all charges. One observes from Fig. 10 that the data points cluster around 0.075 for pp and pA collisions, whereas they lie at about 0.13 for central S+S, S+Ag and Pb+Pb reactions. This represents an enhancement of strangeness production of about a factor 2 in nucleus-nucleus collisions. Note, that kaons represent

over 70% of the total strangeness produced during a collision; therefore, this measurement represents the strangeness content of the system quite well.

Strangeness production is known to be suppressed in pp and pA collisions at this energy. Central nuclear collisions appear to remove this suppression. In fact a partonic state at T>200 MeV is expected to produce nearly equal abundances of the three light flavors in spite of the strange quark being heavier. It will simply coalesce into hadrons during hadronization, resulting in a $\bar{\Lambda}/\bar{p}$ ratio $\approx>1$; indeed, we see a somewhat "corresponding" signal in the data [34]. Fig.11 presents the ratio of $\bar{\Lambda}/\bar{p}$ in central heavy ion collisions from NA35 (S+S, S+Ag, S+Au) and NA49 (Pb+Pb), compared with pp and pA data. Whereas the pp and pA data stay below about 0.4, the S+S, Ag, Au and Pb+Pb ratios average at about unity. This ratio is plotted against mid-rapidity negative hadron multiplicity density. From the flavor composition of $\bar{\Lambda}$ and $\bar{p}$, one intuitively expects that the production ratio reflects the $\bar{s}$:$\bar{u}$ ratio in the source. Moreover, the $\bar{\Lambda}/\bar{p}$ ratio represents a "clean" signal of flavor density in the source as it only refers to newly created antiquarks.

With the observation of $\bar{\Lambda}/\bar{p} \approx 1$ in heavy ion collisions, the crucial question arises: are we seeing a signal of flavour equilibration in the source ? Again, as in previous sections, there is no definite answer to this question. However, the strangeness enhancement (Λ, $\bar{\Lambda}$, K^0) reported originally by NA35/49 was confirmed by the multistrange hyperon yields studied at mid-rapidity in S- and Pb-induced reactions by the WA85/94/97 [35] and NA35/49 [36] collaborations. Figure 12 shows a comparison of the Ξ^-/Λ and $\bar{\Xi}^-/\bar{\Lambda}$ ratios in heavy ion reactions with available pp, $p\bar{p}$, e+e- and pA data. It is clear that multistrange particle production in heavy ion collisions is further enhanced over elementary and pA data. Points for Pb+Pb data are still preliminary and, with large error bars, are compatible with the S+A_T measurements.

This behavior was predicted over 10 years ago [32] for systems which undergo a phase transition and it has been suggested as a signature of the phase transition to a quark-gluon plasma. In the QGP scenario, flavour equilibration, causing possible strangeness enhancement, could be created with in a time interval comparable with the interaction time of the high-energy collision (a few fm/c). Whereas, in a purely hadronic scenario, the establishment of a similar system would require a much longer time (factor ~30 longer). It was expected that the abundant production of hyperons should be more pronounced for multi-strange, than for singly-strange, particles because of the high density of $s\bar{s}$ pairs in the plasma and, because the suppression of strange particle production in hadronic processes increases with growing strangeness content (strong effect on Ξ's and Ω's) due to the higher mass threshold.

Simulations of QCD on the lattice can provide predictions (e.g. [37]) of the strangeness content in a QGP. These predictions, however, require a hadronization model in order to relate them to the experimentally accessible strange particle yields. Results, of course, strongly depend on the chosen model. Numerous studies have been tried, yet none have been able to reproduce all of the measured particle abundances qualitatively [38,39]. Thermal equilibrium models were found to be equally unsuccessful in describing strange particle ratios - they could only reproduce the measurements qualitatively within a factor of two [40]. Numerous attempts were

undertaken to modify string-hadronic approaches in order to reproduce the data. In addition to the standard string scenario, the models included additional processes like secondary hadronic interactions, fusion of strings, collective gluon emission [41,42,43,44], etc. They approximately reproduce the absolute strangeness yield in nucleus-nucleus collisions, but fail to describe the experimentally observed strangeness enhancement, because they can not simultaneously describe strange and non-strange particle production in N+N interactions and central nucleus-nucleus collisions.

7. Summary

Studies of Pb on Pb interactions by CERN SPS experiments demonstrated that the critical values of the QCD phase transition parameters have been reached, and exceeded, in the extended high energy density volumes of the analyzed collisions. Thus the crucial question arises: is the quark-gluon plasma already being created in central nucleus-nucleus collisions at 158 GeV/c ? There is no definite answer to this question, but analysis of the recent data provided a number of suggestive "hints" that the hadronic scenario, which worked satisfactorily at lower energies, does NOT describe Pb+Pb collisions. This includes:

1. Evidence of an approach to chemical equilibrium in heavy ion collisions (strangeness enhancement in all investigated channels, including hidden strangeness - Φ meson [45]).
2. Signals associated with the possible chiral symmetry restoration mass loss in both leptonic channels e+e- and μ+μ- (the description of the low mass dilepton enhancement in the vector meson domain seems to require an in-medium mass loss of the vector mesons).
3. Indication of the existence of a partonic phase from J/Ψ production data.

With the present, very qualitative, level of understanding, the CERN SPS heavy ion data seems to signal a sudden phase change. We are entering an entirely new frontier "where no man has gone before" ...

Acknowledgment: This work was supported by the Director, Office of Energy Research, Office of Basic Energy Sciences, Nuclear Sciences Division, of the U.S. Department of Energy under Contract No. DE-AC03-76SF00098.

References:

1. e.g. Proceedings of Quark Matter'96 Conference, Nucl.Phys. A610 (1996)
2. C.Bernard et al., Thermodynamics for two flavor QCD, hep-lat 9608026
   for review, see: E.Laermann, Nucl.Phys. A610 (1996) 1c
3. T.Alber et al. (NA49 Coll.), Phys.Rev.Lett. 75 (1995) 3814
4. A.Pfeiffer et al. (NA45 Coll.), Proc. ICHEP'96

5. M.Gonin et al. (NA50 Coll.), Nucl.Phys. A610 (1996) 404c
6. I.Kralik et al. (WA97 Coll.), Proc. QM'97 Conf., Dec.97, Tsukuba, Japan
7. G.Ambrosini et al. (NA52 Coll.) - BUHE 97-05, to be published in Phys.Lett.B
8. T.Peitzmann et al. (WA98 Coll.), Nucl.Phys. A610 (1996) 200c
9. P.Jones et al. (NA49 Coll.), Nucl.Phys. A610 (1996) 188c
10. G.Roland et al. (NA49 Coll.), Proc. QM'97 Conf., Dec.97, Tsukuba, Japan
11. J.D.Bjorken, Phys.Rev.D27 (1983) 140
12. S.Margetis et al. (NA49 Coll.), Nucl.Phys. A590 (1995) 335c
13. D.Karzeev, Nucl.Phys. A610 (1996) 418c
14. J.P.Blaizot and J.Y.Ollitrault, Nucl.Phys. A610 (1996) 452c
15. T.Matsui and H.Satz, Phys.Lett. B178 (1986) 416
16. H.Satz, Nucl.Phys. A590 (1995) 63c
17. M.C.Abreu et al. (NA38 Coll.), Nucl.Phys. A566 (1994) 77c
S.Ramos et al. (NA38 Coll.), Nucl.Phys. A590 (1995) 117c
18. P.L.McGaughey et al. (E722 Coll.), Phys.Rev. D50 (1994) 3038
19. C.Gerschel and J.Hufner, Z.Phys. C56 (1992) 171
20. E.Braaten and S.Fleming, Phys.Rev.Lett. 74 (1995) 3327
21. D.Kharzeev and H.Satz, Phys.Lett. B366 (1996) 316
22. G.Agakichiev et al. (NA45 Coll.), Nucl.Phys. A610 (1996) 317c
23. G. Agakichiev et al., Phys.Rev.Lett. 75 (1995) 1272
24. P.Wurm et al., Nucl.Phys. A590 (1995) 103c
25. G.Q.Li, C.M.Ko and G.E.Brown, Phys.Rev.Lett. 75 (1995) 4007
26. W.Cassing, W.Ehehalt and C.M.Ko, Phys.Lett. B363 (1995) 35
27. V.Koch and C.Song, preprint LBL-38619 UC 413
28. D.K.Srivastava et al., Phys.Rev. C53 (1996) 567
29. J.Sollfrank et al., Preprint nucl-th/9607029 (1996)
30. R.Baier and K.Redlich, private communication
31. C.M.Ko et al., Nucl.Phys.A610 (1996) 342c
32. C.Bormann et al. (NA49 Coll.), Proc. of Strangeness in Quark Matter'97, April 1997, Santorini, Greece
33. P.Koch, B.Muller and J.Rafelski, Phys.Rep. 142 (1986) 167
J.Latessier, J.Rafelski and A.Tounsi, Phys.Lett. B333 (1994) 484
J.Latessier, J.Rafelski and A.Tounsi, Phys.Lett. B390 (1997) 363
J.Latessier, J.Rafelski and A.Tounsi, Phys.Lett. B410 (1997) 315
34. T.Alber et al., Phys.Lett. B366 (1996) 56
35. H.Helstrup et al. (WA97 Coll.), Nucl.Phys. A610 (1996) 165c
H.Sandor et al. (WA97 Coll.), Proc. of XXVI International Symposium on Multiparticle Dynamics, Fero 1996, Portugal
A.Jacholkowski et al. (WA97 Coll.), 1997, Jerusalem, Israel
36. G.Odyniec et al. (NA49 Coll.), Proc. of Strangeness in Quark Matter'97, April 1997, Santorini, Greece
37. J.Kogut and D.Sinclair, Phys.Rev.Lett. 60 (1988) 1250
38. H.Barz et al., Nucl.Phys. A519 (1990) 831
39. U.Ornik et al., Phys.Rev. C54 (1996) 1381
40. P.Braun-Munzinger et al., Phys.Lett. B365 (1996)
J.Stachel, Nucl.Phys. A610 (1996) 509c

41. A.Tai, B.Anderson and Ben-Hao Sa, Proc of International Conference Strangeness'95 January 4-7, 1995, Tucson, Arizona
42. N.S.Amelin et al., Phys.Rev. C47 (1993) 2299
43. N.Armesto, Report of Universidade de Santiago de Compostela, US-FT/16-94(1994)
44. B.Anderson et al., Lund Report LU-TP-87-6 (1987)
B.Anderson et al., Z.Phys. C57 (1993) 485
45. V.Friese et al. (NA49 Coll.), Proc. of Strangeness in Quark Matter'97, April 1997, Santorini, Greece
46. N.Xu et al. (NA44 Coll.), Nucl.Phys. A610 (1996) 175c

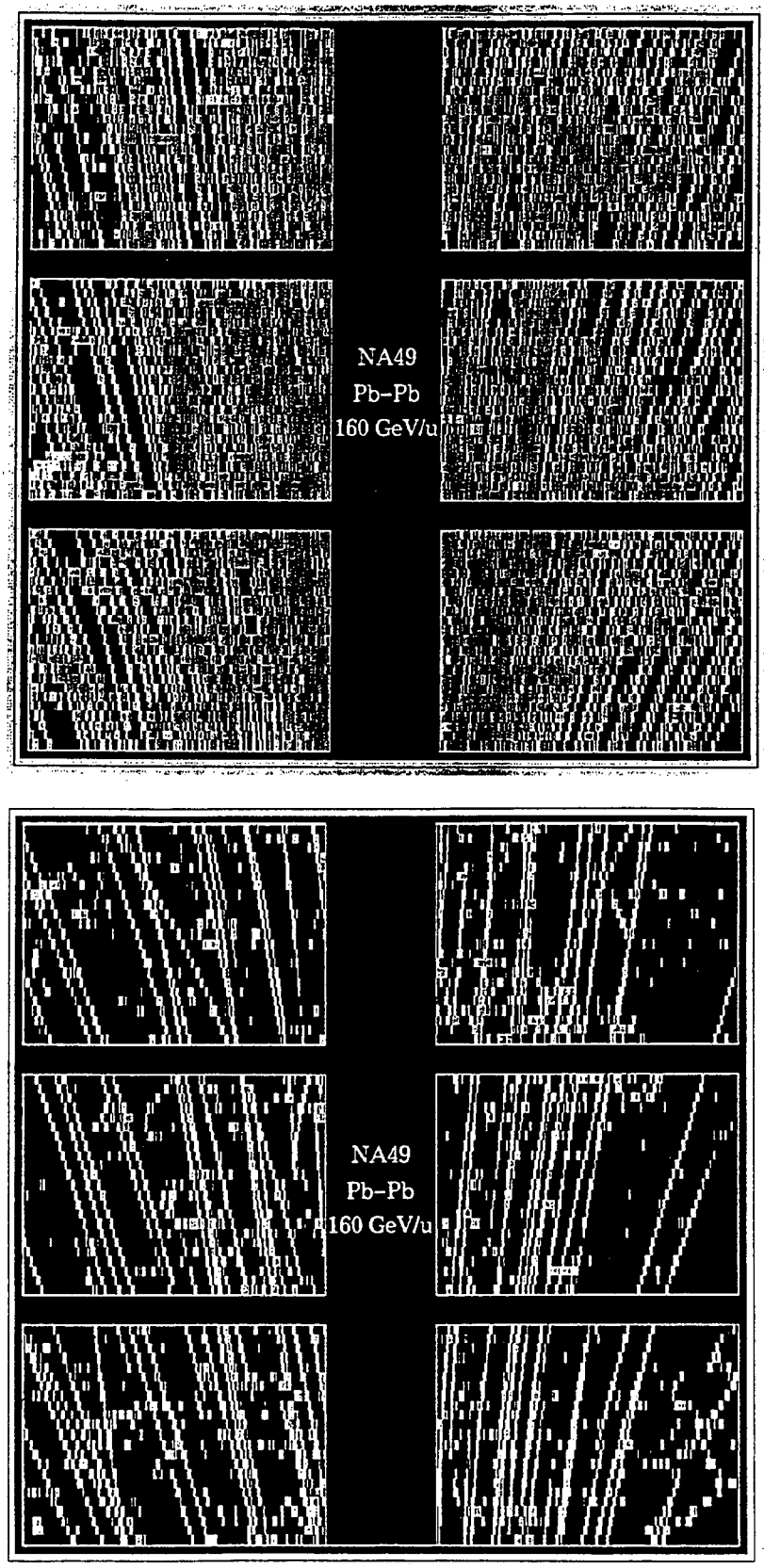

Figure 1. Charged particle tracks in a central Pb+Pb event recorded by the vertex TPC of the NA49 experiment. The top panel displays the full depth of the detector (30 cm); the lower one, a subvolume of 5 cm depth.

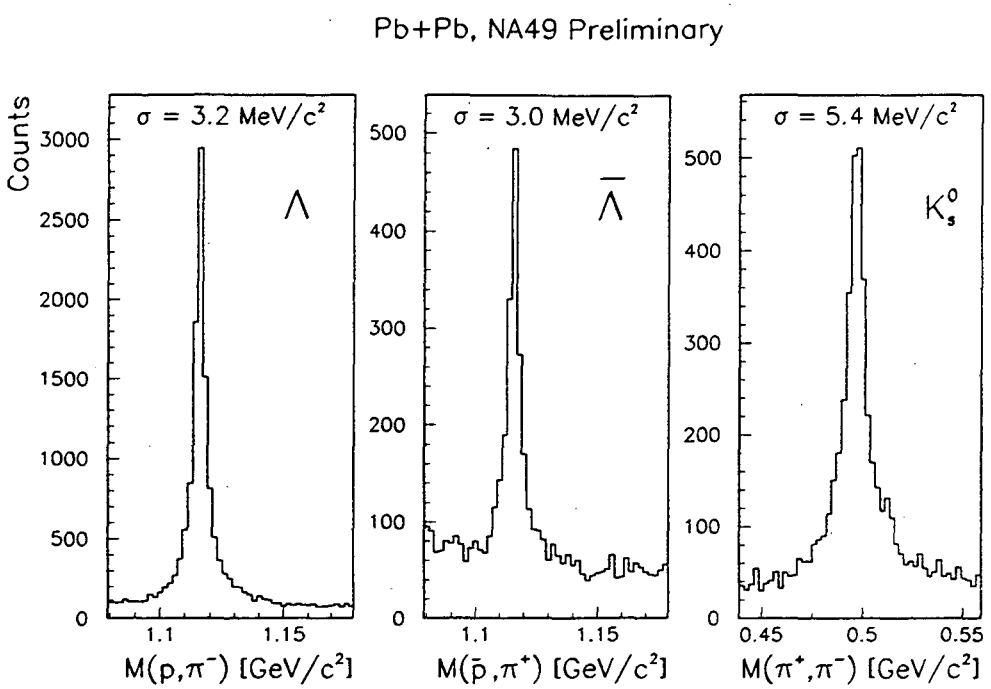

Figure 2. The Λ, $\bar{\Lambda}$ and K^0 invariant-mass distribution obtained by the NA49 experiment.

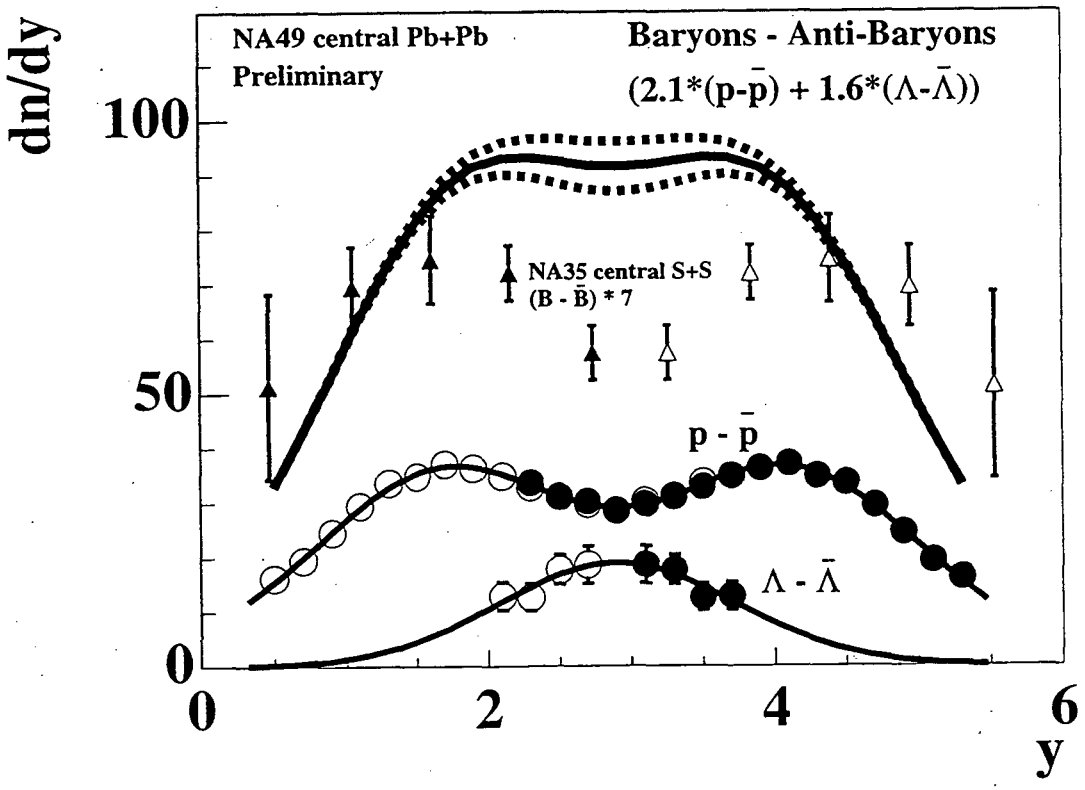

Figure 3. Net baryon density for central Pb+Pb and S+S collisions measured by the NA35/49 experiment. For comparison net proton and net Λ distributions are shown (see text). Full symbols represent measurements, open ones reflect points around mid-rapidity.

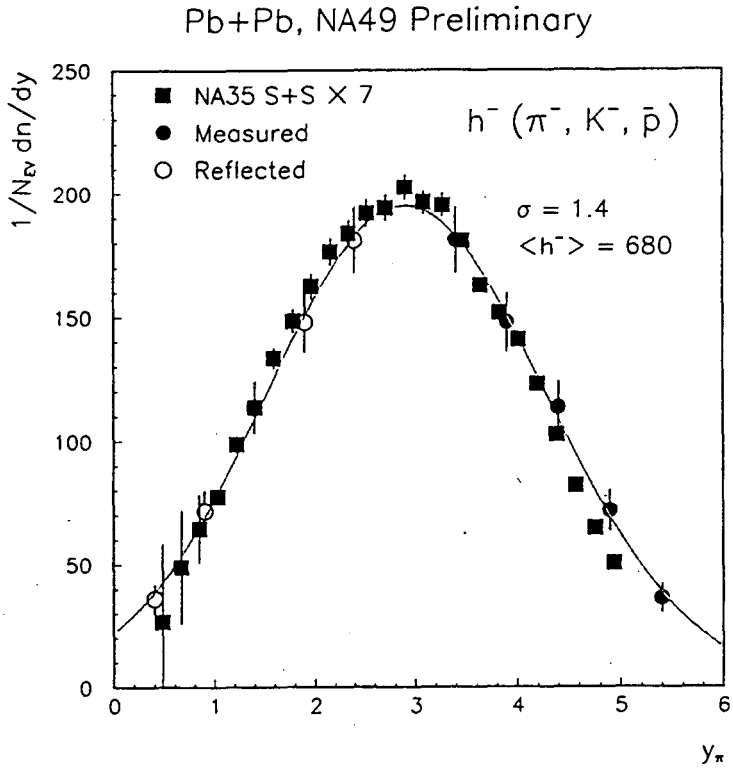

Figure 4. Rapidity distribution for negative hadrons in Pb+Pb collisions (NA49 experiment) and for S+S collisions (NA35 experiment) scaled for comparison by the ratio of participants in both systems.

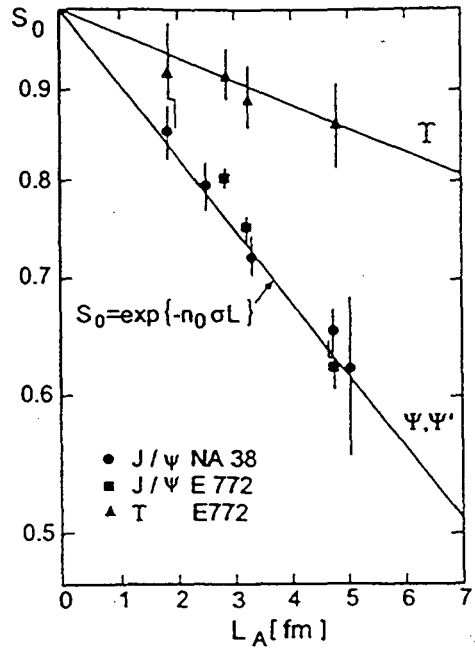

Figure 5. Quarkonium attenuation in J/Ψ and Ψ' production on nuclear targets of increasing size. L_A (see text) is an average length (Glauber trajectory) traversed by initially produced $c\bar{c}$ pairs in a nuclear target.

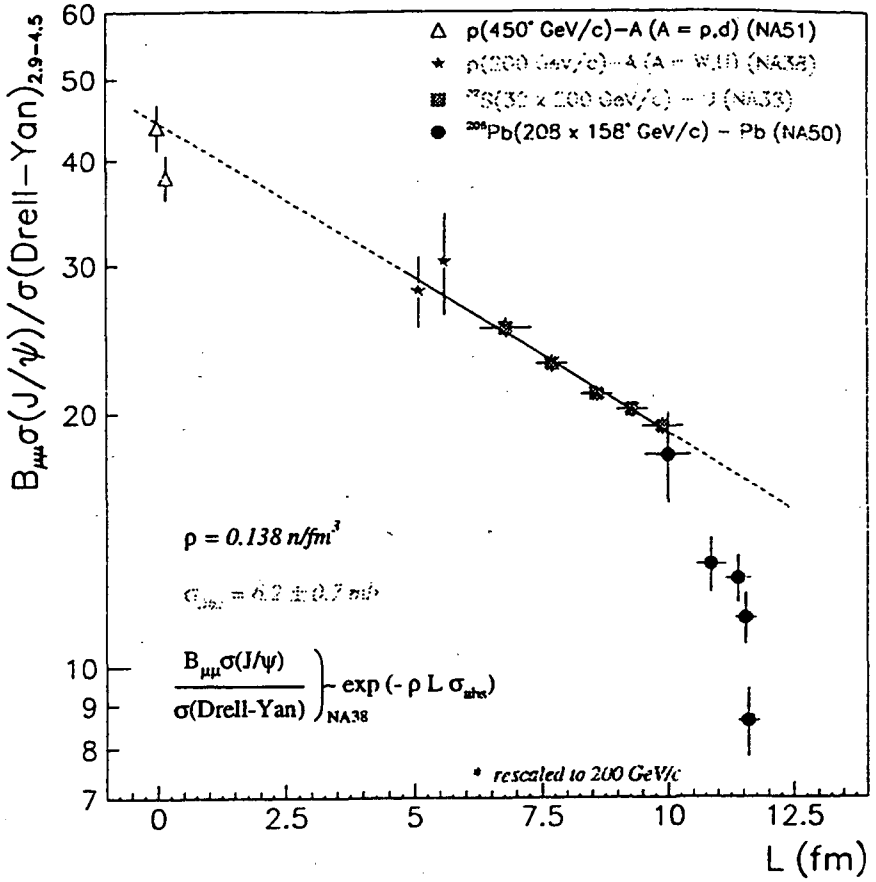

Figure 6. J/Ψ production in proton-, sulfur- and lead-induced collisions from the NA38/50/51 experiments. For a description of the fit - see text.

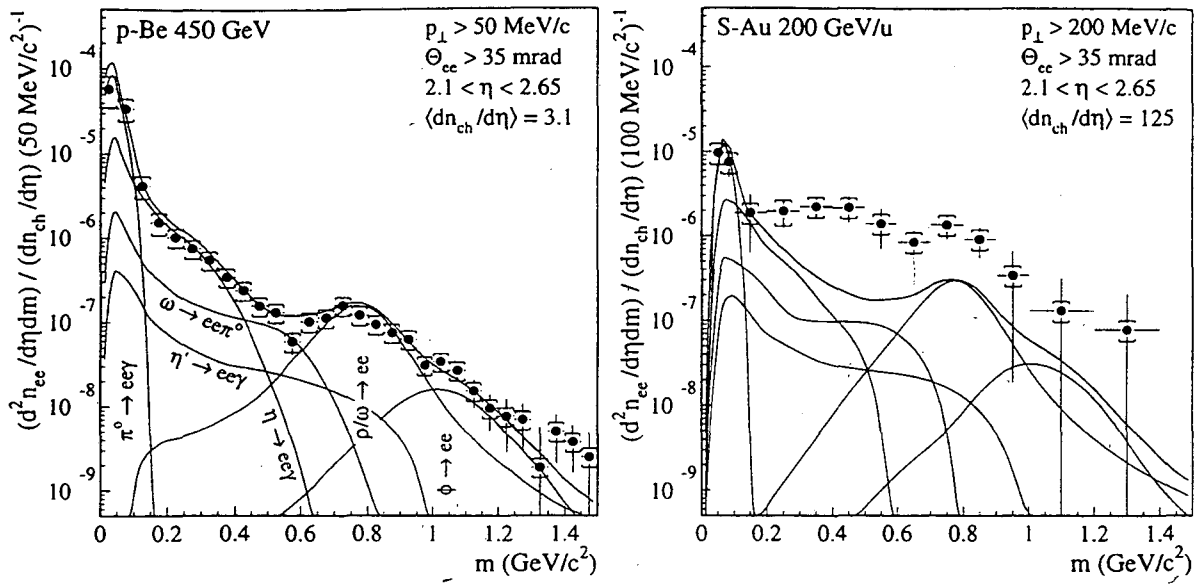

Figure 7. Mass spectra of inclusive e+e- pairs in 450 GeV p+Be (left) and S+Au (right) collisions showing the data (full circles) and various contributions from hadronic decays. Systematic (brackets) and statistical (bars) errors are plotted independently of each other.

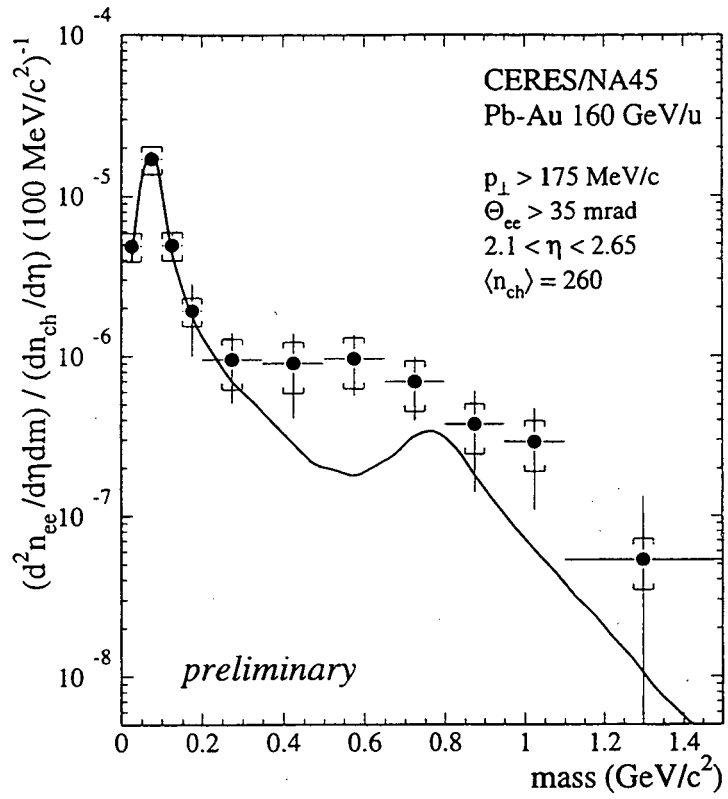

Figure 8. Preliminary mass spectrum of inclusive e+e- pairs in 158 GeV/c Pb+Au collisions (NA45 experiment). Systematic (brackets) and statistical (bars) errors are plotted independently of each other. The solid lines show the summed contributions from hadron decays.

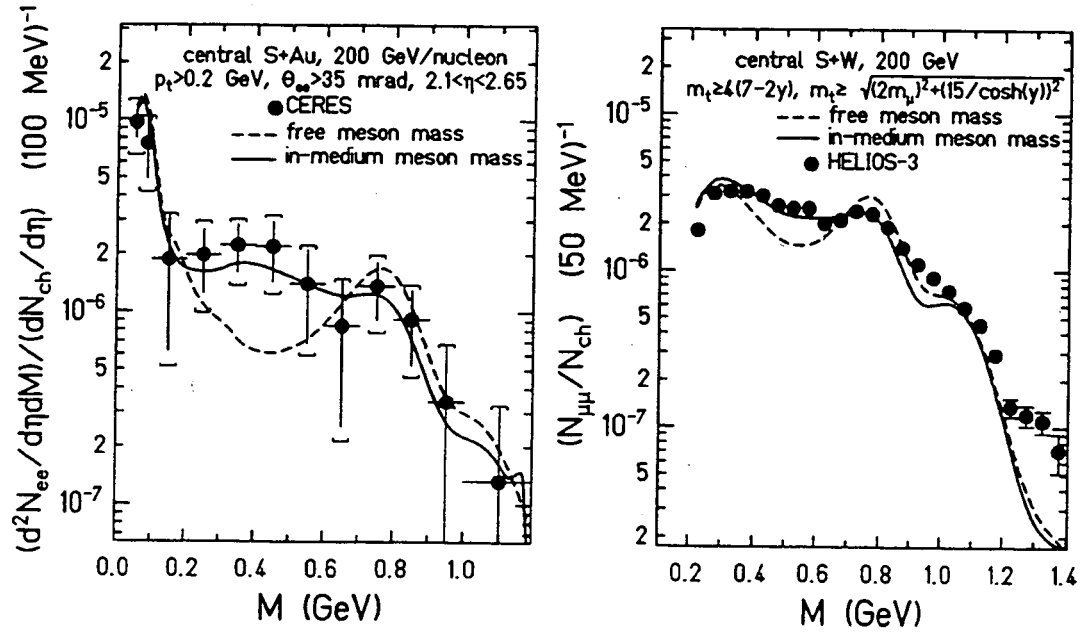

Figure 9. Dilepton invariant-mass spectra in (a) S+Au (e+e- from NA45) and (b) S+W (μ+μ– from HELIOS/3) collisions at 200 GeV/c. Solid curves represent calculations of the in-medium vector meson masses.

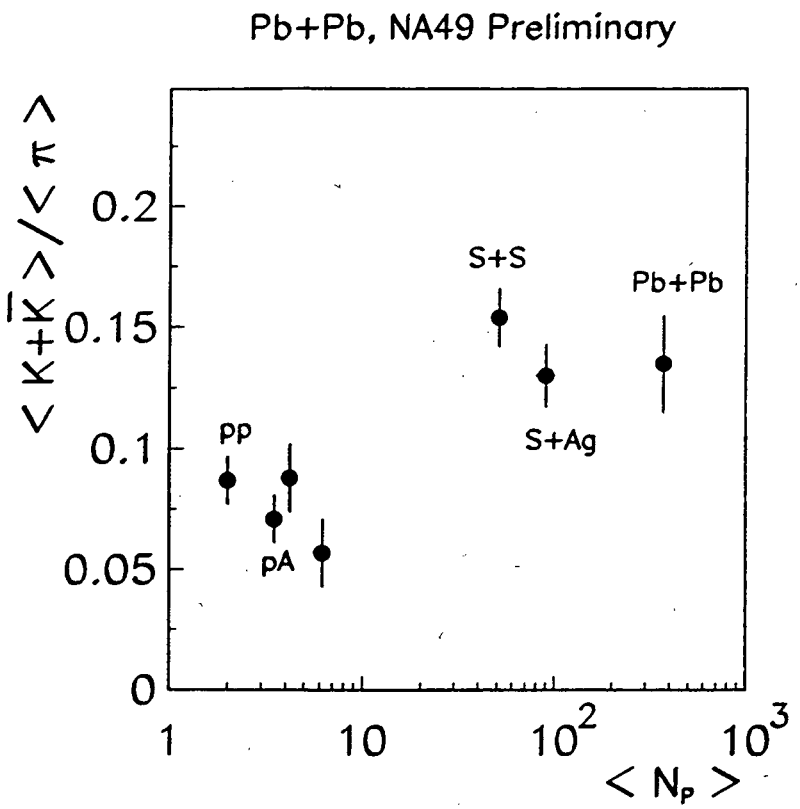

Figure 10. The dependence of the K/π ratio, defined as the sum of the multiplicities of all kaons (K^+, K^-, K_s^0) divided by all pions (π^+, π^-, π^0), on the number of participant nucleons.

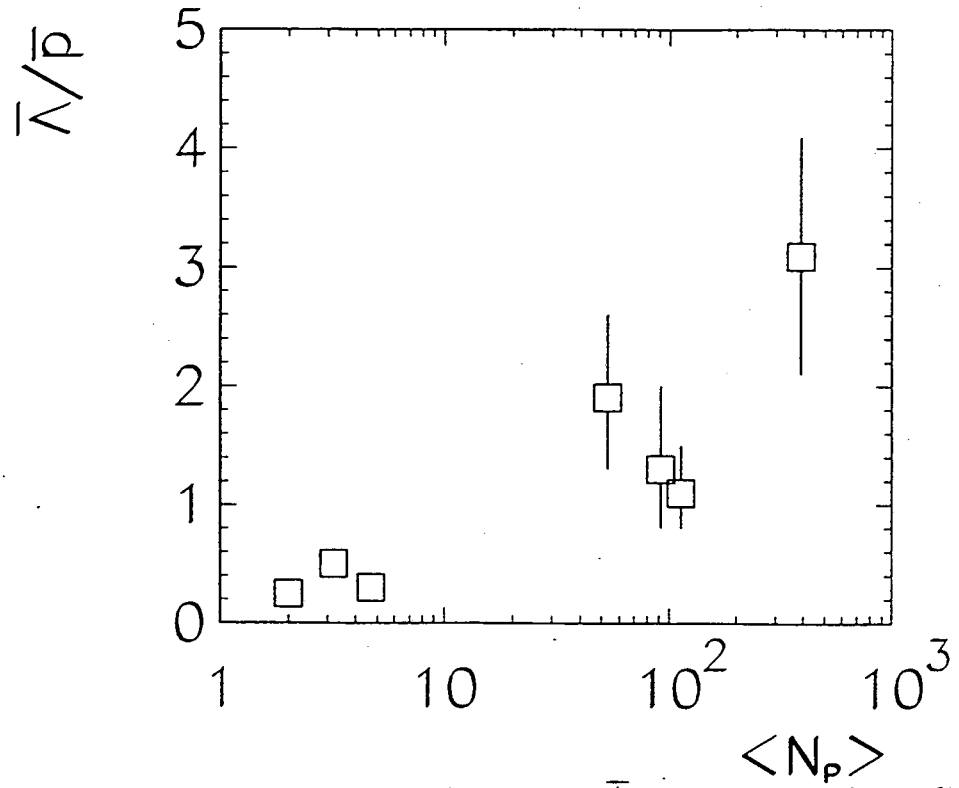

Figure 11. Ratio of the rapidity densities of $\bar{\Lambda}$ and $\bar{p}$ near mid-rapidity for various target-projectile systems as a function of the number of participants.

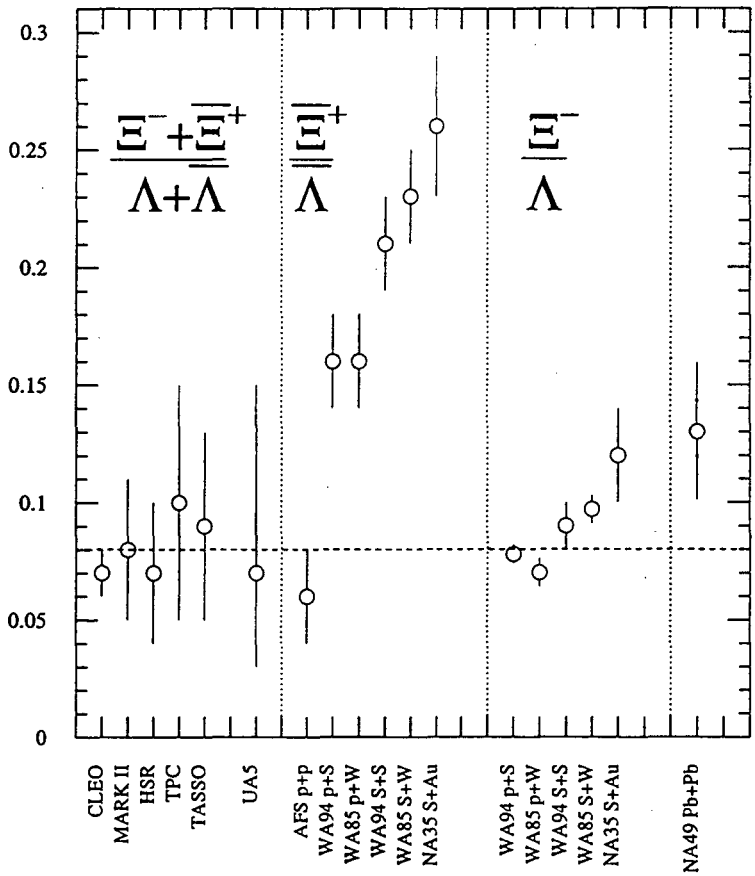

Figure 12. Ratio of multi-strange baryon-antibaryon particle abundances, measured in the central rapidity region at 200 GeV/c (S+S/W/Au collisions) and 158 GeV/c (Pb+Pb collisions) compared to ratios obtained in lepton- and nucleon-induced reactions.

Ernest Orlando Lawrence Berkeley National Laboratory
One Cyclotron Road | Berkeley, California 94720

Prepared for the U.S. Department of Energy under Contract No. DE-AC03-76SF00098